INELASTIC BEHAVIOR OF HIGH STRENGTH STEEL FRAMES SUBJECTED TO CONSTANT VERTICAL AND ALTERNATING HORIZONTAL LOADS

by Chiaki MATSUI[I] and Isao MITANI[II]

Synopsis In order to clarify the restoring force characteristics of high strength steel frames, portal frame specimens were tested under constant vertical and alternating horizontal loads, the vertical load ratio and mechanical properties of steel material being varied. It has been shown that the results of analysis predict well the experimental behavior, including the upper limit value of the load carrying capacity, the plastic energy absorption capacity and the amount of plastic strain accumulated in the section.

Introduction It is well recognized that the dynamic analysis is needed to evaluate the overall resistance of structures to the strong earthquake disturbances, and the hysteretic restoring force characteristics of different types of structural members and structures have been studied experimentally and theoretically. The hysteretic behavior of steel frames has also been extensively studied, the mild steel being the main material.

When to design a structure under a prescribed design load, the economical design may require the use of high strength steel, since it reduces the weight of the structural members. In Japan, the law permits the use of high strength steel in the structures designed based on the allowable stresses. In order to extend this advantage to the plastic design, the investigations have been reported on the limiting values of width-to-thickness ratio of plate elements composing cross sections and on the spacing of braces to prevent the lateral buckling of members. However, very few research can be found on the hysteretic restoring force characteristics of high strength steel frames under alternating horizontal load resulted from the earthquake[1].

The mechanical property of high strength steel shows that the strain-hardening effect is not much expected due to the high ratio of the yield stress σ_y to the maximum tensile strength σ_u, and the extensibility is rather small, in comparison with mild steel. It is needed to clarify the effects of these properties on the restoring force characteristics, especially on the energy absorption capacity of the frame, which is the significant measure representing the resistance of the frame to the earthquake disturbances.

In the present study, portal frame specimens manufactured from three different steel materials, i.e., two different high strength steels and a mild steel were tested under constant vertical and alternating horizontal loads. Results are compared with theoretical predictions obtained from the analysis taking the characteristics of high strength steel into account.

Test program Test program consists of three series, steel materials used in each series being as follows; mild steel SM41(nominal yield stress $\sigma_y \geqq 2.5$ t/cm^2, nominal maximum tensile strength σ_u = 4.1-5.2 t/cm^2) in Series I, and high strength steel SM50($\sigma_y \geqq 3.3$ t/cm^2, σ_u = 5.0-6.2 t/cm^2) and SM58 ($\sigma_y \geqq 4.7$ t/cm^2, σ_u = 5.8-7.3 t/cm^2) in Series II and III, respectively, specified by Japanese Industrial Standard. Each series contains three portal frame specimens assembled by welding from built-up H-shape steel members, details of a specimen being shown in Fig. 1. In all specimens, beam-to-column connection panels are stiffened by two steel plates of 6 mm thickness and protected against shear failure. Column base and beam ends of specimens in

I) Assoc. Prof., Faculty of Engineering, Kyushu Univ., Fukuoka, Japan.
II) Lecturer, Faculty of Engineering, Kagoshima Univ., Kagoshima, Japan.

Series III are also stiffened by 6 mm thick cover plates. Out-of-plane deformations are prevented at two column tops and two quarter points of beam. The value of the vertical load on each frame specimen and mechanical property of steel material are shown in Table 1. The ratios of the vertical load P to the yield load of the column P_y are taken equal to 0.1, 0.25 and 0.5.

Figure 2 shows the loading apparatus whose working principle is explained in detail in Ref. 2. The frame specimen is first subjected to the vertical load P which is kept constant during the test, and then 10 cycles of alternating horizontal load H is applied at the level of beam-to-column connection, amplitude of Δ/h, the ratio of the horizontal displacement at column top Δ to the column height h, being constantly kept equal to $\pm 1.5/100$. After that, additional cycles of horizontal loading were done with the amplitude of Δ/h equal to $\pm 3.0/100$, until the carrying capacity was reduced to 90% of the maximum value that the specimen had experienced. The strains were recorded at each load level, whose locations are shown in Fig. 1.

Test Results The relation between H and Δ obtained in the tests are shown in Fig. 3, where only typical hysteretic loops are drawn to avoid the confusion, numbers indicating the loading cycle counted by each half cycle. Figure 4 shows the relation between the value of H at turning points and the number of loading cycles, where the occurrences of local buckling, out-of-plane deformation and cracks in the welded portion are indicated.

The following observations are made from the test results:
a) Behavior during the loading with the amplitude Δ/h equal to $\pm 1.5/100$: Instability point does not appear in any of specimens tested, and the spindle-shape hysteretic loops are obtained. The hysteretic loop of specimens under the vertical load ratio n, which is P/P_y, equal to 0.1 and 0.25 stabilizes after 2/2 cycle of loading, while that under n = 0.5 stabilizes after 10/2 to 16/2 cycles, the carrying capacity gradually increasing in each cycle of loading. The effect due to the difference in steel is not visibly observed.

b) Behavior during the loading with the amplitude Δ/h equal to $\pm 3.0/100$: Specimens under n equal to 0.1 show the spindle-shape hysteretic loops, instability point being not observed. The reduction of carrying capacity occurs due to the propagation of cracks at beam ends, except for specimen II-1. In case of specimens under n equal to 0.25, instability point is observed in the first loading cycle (20/2 cycle), but it disappears with the increase in the carrying capacity in the following cycles of loading. Propagating cracks at beam ends cause the reduction of the carrying capacity. Specimens under n equal to 0.5 show clearly the unstable portion in the hysteretic loops obtained after 20/2 cycles of loading, and the increase in the carrying capacity is not much expected. The reduction occurs due to out-of-plane deformation associated with twisting of columns. As for the effect due to the difference in steel material, it is observed that the reduction of carrying capacity occurs earlier in specimens with larger values of σ_y/σ_u.

Figure 5 shows the relation between the strain at the column base measured at turning points and the number of loading cycles. It is observed from the strain data of specimens with small values of σ_y/σ_u and n that the strain tends to converge. Specimens of the same steel show that the increase in the strain is larger as the value of n increases, and if the n-value is the same, the increase in the strain is larger in specimens with larger value of σ_y/σ_u.

Theoretical Prediction and Discussion The moment-curvature relations are theoretically computed from the idealized hysteretic stress-strain relation

shown in Fig. 6, where $\eta = \sigma/\sigma_y$, $\xi = \varepsilon/\varepsilon_y$, σ and ε denote the stress and strain respectively, ε_y the yield strain. The ratio σ_u/σ_y is denoted by α, and the slope of the curve in the strain-hardening range by μ. Figures 7(a) and (b) show non-dimensional moment-curvature, m-ϕ, relations obtained by assuming that the cross section is ideal sandwich section and plane remains plane after the deformation takes place. m and ϕ are defined as $m = M/M_y$ and $\phi = \Phi/\Phi_y$, where moment M and curvature Φ are non-dimensionalized by their respective values at yield limit. Note that the value of m will converge to the value given as follows, in accordance with the values of n and α:

$$m = \tau_0(\phi \mp 1) \pm 1 \quad \text{if } \alpha - n > 1 \; ; \quad m = \pm(\alpha - n) \quad \text{if } \alpha - n \leqq 1 \qquad (1a,b)$$

where $\tau_0 = 2\mu$. Before the hysteretic loop converges to the one given by Eqs. (1a,b), it follows the elastic recovery line until the value of m reaches the value at turning point of the previous cycle. The relation shown in Fig. 7(a) was already used in the analysis performed in Ref. 3.

Load-Displacement Relations The deflections of portal frames tested are analysed by numerical integration based on the previously established m-ϕ relations, bending and shear deformations of members and shear deformation of beam-to-column connection panels being taken into account[4].

Dotted lines in Fig. 3 indicate the hysteretic H-Δ relations obtained from the analysis. Only two loops are shown for the loading with the amplitude Δ/h equal to $\pm 3.0/100$, and this means that the theoretical hysteresis loops stabilize after two cycles of loading. The theory predicts well the experimentally observed phenomena, i.e., the convergence of the loops and the increase in the carrying capacity with the increase in the loading cycle. However, the discrepancy is observed to be large in the transitional region between the elastic and plastic behaviors, due to the neglect of Bauschinger effect and the idealization of the cross section.

Upper Limit of Load Carrying Capacity It is already indicated in Figs. 3 and 4 that the hysteretic H-Δ loops converge to a certain loop in the large displacement range. Therefore, the upper limit of the load carrying capacity can be directly predicted from Eqs.(1a,b), in accordance with the collapse mechanism of the frame. Dashed lines in Fig. 3 are the collapse mechanism lines obtained in such a manner. For comparison, two additional mechanism lines based on the full plastic moment M_p and the reduced full plastic moment M_{pc} due to the axial force in columns are shown by dash-dotted and dotted lines, respectively. M_p is the converged value of the moment carrying capacity of the section under $n \neq 0$ on the assumption that $\sigma_u = \infty$, and in fact it corresponds to the case where $n = 0$. Figure 3 shows a good correlation between the mechanism lines based on Eqs. (1a,b) and the maximum load carrying capacities obtained in the tests.

Converged Value of Accumulated Strain Consider the stress-strain relation shown in Fig. 8, where the plastic flow is taken into account, in order to derive the condition for the strain at the centroid of the ideal sandwich section to converge to a certain value under constant axial force and alternating bending. At the stage in which the strain at centroid converges to a certain value, the cross section behaves in such a way that the amount of the plastic strain generated in one flange is equal in opposite direction to that in the other flange under the combined action of the constant axial force and bending. Such behavior is possible only when the stress and strain in the flexural tension flange are on the line BC, and those in compression flange on the line B'C'. Thus, the conditions required are as follows:

$$\alpha - n > 1 \quad \text{and} \quad \phi < 1 - (1 - \alpha + n)/\mu \tag{2}$$

The value of converged strain is given at point X in Fig. 8, as follows:

$$\xi = n/\mu + \xi_{st} + 1 \tag{3}$$

where ξ_{st} is the value of $\varepsilon/\varepsilon_y$ at the start of the strain-hardening. The values of the converged strains at centroid of the cross section obtained from Eq.(3) are indicated in Fig. 5 by dash-dotted lines. A good agreement is observed between the theoretical and experimental results of specimens in Series I. Discrepancy observed in Series III is due to the fact that the strain data have not been taken at the point of the maximum bending moment along the column length, as shown in Fig. 1.

Plastic Energy Absorption Capacity Figure 9 shows the relation between the accumulated energy ΣW and plastic displacement $\Sigma\Delta_{PA}$. When to evaluate W and Δ_{PA} in each cycle of loading, only hysteretic loops are taken in which the carrying capacity sustains 95 or 90% of the value of the maximum load carrying capacity that the specimen has experienced. Comparing the results obtained for specimens of the same steel material, it is known that the values of ΣW and $\Sigma\Delta_{PA}$ decrease quite drastically due to the axial load effect.

In Fig. 10, ΣW and $\Sigma\Delta_{PA}$ are non-dimensionalized by H_{PN} and Δ_{PN}, respectively, which are the load and displacement at the intersection of the elastic line and the collapse mechanism line, as shown in the figure. From Fig. 10, it may be pertinent to say that the advantageous property of the material is not properly utilized in high strength steel frames designed expecting the elastic-plastic behavior under the strong earthquake motion, and their performance may not be better than that of mild steel frames.

Summary and Conclusion Investigated experimentally and theoretically are the restoring force characteristics of portal frames with various material properties and various vertical load ratios under alternating horizontal loading. It has been shown that the present theory can predict well the upper limit of the load carrying capacity and the converged value of the strain in the cross section of the column. It may be concluded from the results concerning the plastic energy absorption capacity that the high strength steel frames should be carefully designed against the strong earthquake motion, and they are not necessarily better than the mild steel frames in view of seismic design.

References

1) Arnold, P., Adams, P.F. and Lu, L.W., "The Effects of Instability on the Cyclic Behavior of a Frame", Reports , RILEM International Symposium on the Effects of Repeated Loading of Materials and Structures, Mexico, Vol. 6, Sept. 1966.
2) Wakabayashi, M., Nonaka, T. and Matsui, C., "An Experimental Study on the Horizontal Restoring Forces in Steel Frames under Large Vertical Loads", Proc., 4WCEE, Santiago, Vol.I, B-2, Jan. 1969, pp. 117-193.
3) Wakabayashi, M., Matsui, C., Minami, K. and Mitani, I., "Inelastic Behavior of Steel Frames Subjected to Constant Vertical and Alternating Horizontal Loads", Proc., 5WCEE, Rome, Vol.I, June 1973, pp. 1194-1197.
4) Wakabayashi, M., Matsui, C., Minami, K. and Mitani, I., "Inelastic Behavior of Full-Scale Steel Frames with and without Bracings", Bulletin, Disaster Prevention Research Institute, Kyoto Univ., Vol.24, Part 1, Mar. 1974, pp. 1-23.

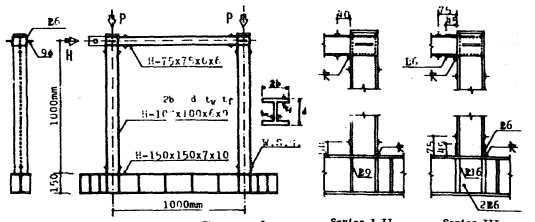

Fig.1 Frame Specimen

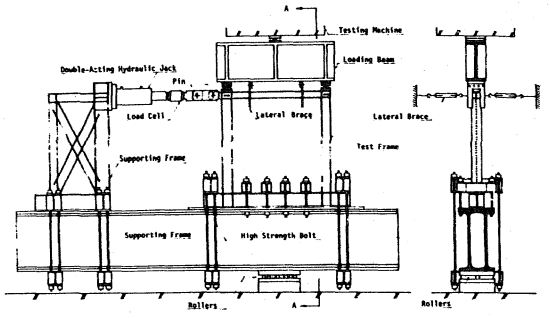

Fig.2 Loading Apparatus

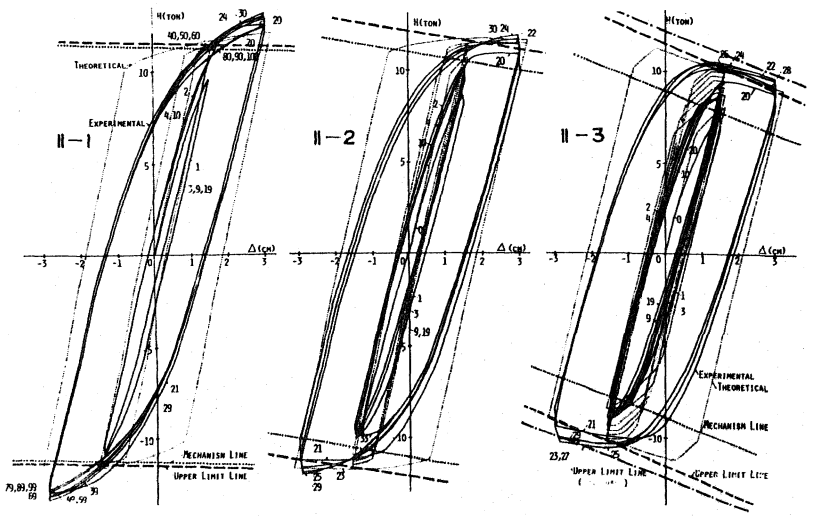

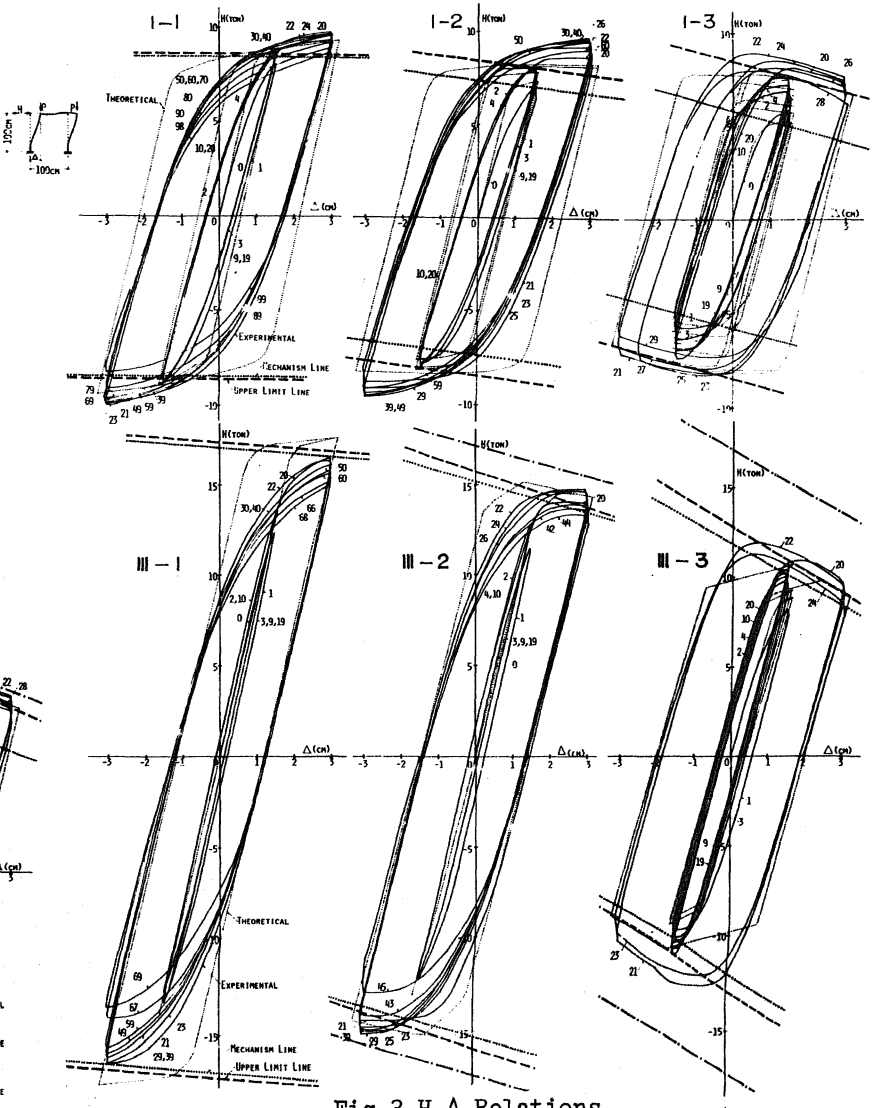

Fig.3 H-Δ Relations

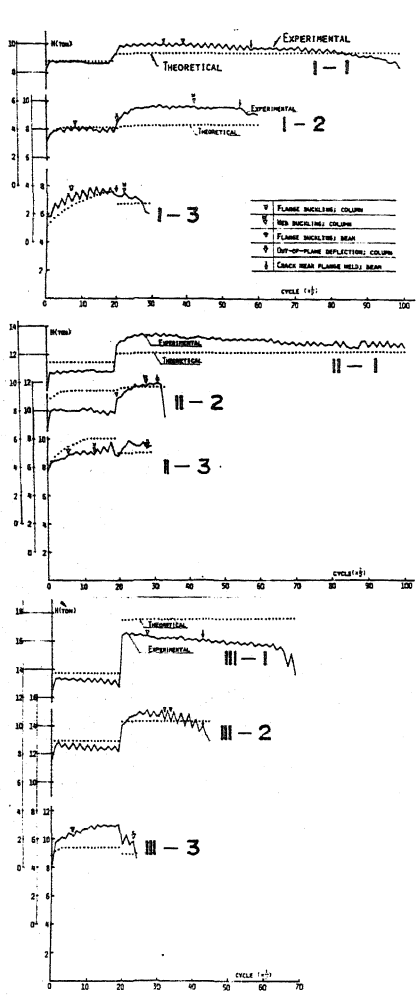

Fig.4 Load H at Turning Points

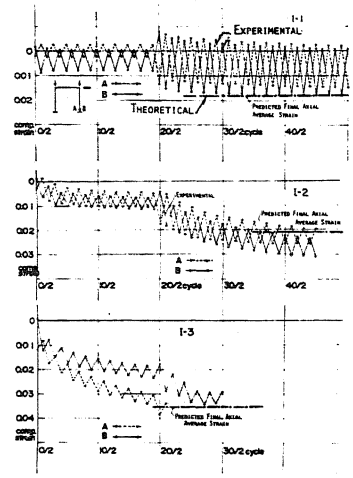

Fig.5 Strain Behavior

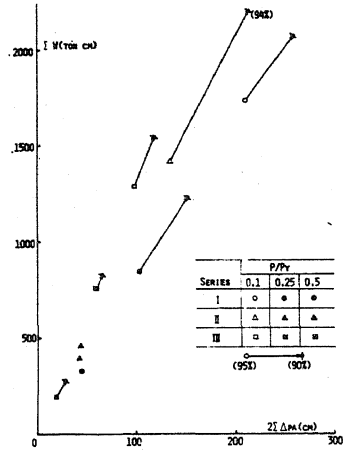

Fig.9 ΣW-$\Sigma\Delta_{PA}$ Relations

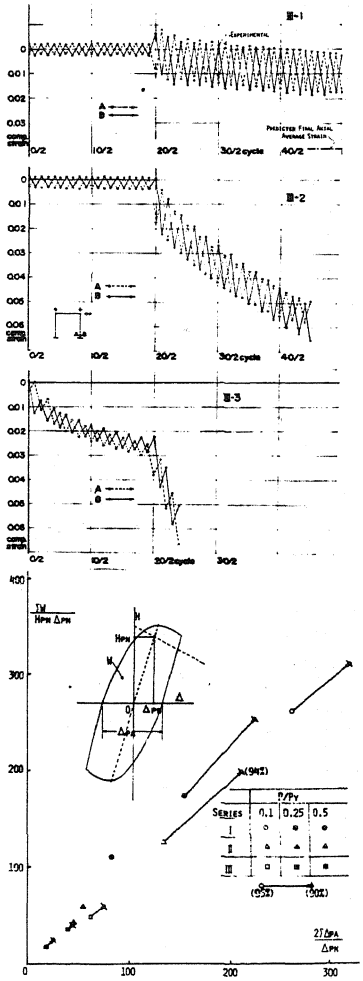

Fig.10 Dimensionless ΣW-$\Sigma\Delta_{PA}$ Relations

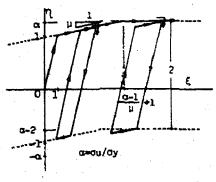

Fig.6 η-ξ Relation

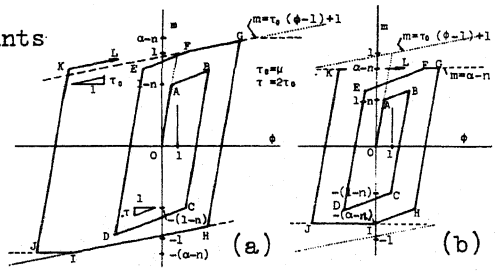

Fig.7 m-ϕ Relations

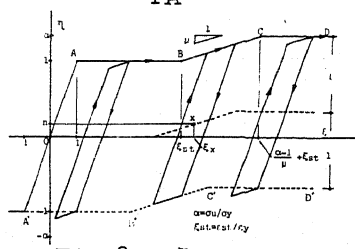

Fig.8 η-ξ Relation

Table 1 Loading Condition and Material Properties

Specimen	P (ton)	P/Py	P/Pe	Material	Column Flange Plate 9 mm					Column Web and Beam Plates 6 mm				
					σ_y (t/cm²)	σ_u (t/cm²)	σ_y/σ_u	$\varepsilon_{st}/\varepsilon_y$	Est/E (%)	σ_y (t/cm²)	σ_u (t/cm²)	σ_y/σ_u	$\varepsilon_{st}/\varepsilon_y$	Est/E (%)
I - 1	6.3	0.10	0.014	SM41	2.74	4.45	0.616	10.0	2.22	2.96	4.38	0.676	10.0	1.80
I - 2	18.0	0.26	0.039		2.93	4.61	0.636	5.4	2.57	2.45	3.91	0.627	6.0	1.27
I - 3	35.8	0.53	0.077		2.93	4.61	0.636	5.4	2.57	2.45	3.91	0.627	6.0	1.27
II - 1	8.8	0.10	0.018	SM50	3.56	5.45	0.650	8.8	2.13	3.57	5.29	0.674	9.8	2.18
II - 2	22.3	0.25	0.045		3.78	5.30	0.713	11.2	1.87	3.85	5.17	0.745	5.5	1.59
II - 3	44.0	0.48	0.090		3.78	5.30	0.713	11.2	1.87	3.85	5.17	0.745	5.5	1.59
III - 1	14.5	0.11	0.031	SM58	5.52	6.28	0.880	6.0	1.06	5.33	6.07	0.878	12.8	1.63
III - 2	35.5	0.26	0.076		5.52	6.28	0.880	6.0	1.06	5.33	6.07	0.878	12.8	1.63
III - 3	69.5	0.51	0.149		5.52	6.28	0.880	6.0	1.06	5.33	6.07	0.878	12.8	1.63

P : vertical load P_y : yield axial load of column $2P_e$: elastic buckling load of frame
σ_y : yield stress σ_u : maximum tensile strength ε_y : yield strain ε_{st} : strain at start of strain hardening
E : modulus of elasticity Est : strain hardening modulus